Influence of Clay Content on the Melting Behavior and Crystal Structure of Nonisothermal Crystallized Poly(L-lactic acid)/Nanocomposites

F. Ublekov,[1] J. Baldrian,[2] J. Kratochvil,[2] M. Steinhart,[3] E. Nedkov[1]

[1]*Institute of Polymers, Department of Structure and Properties of Polymers, Bulgarian Academy of Sciences, Sofia, Bulgaria*
[2]*Institute of Macromolecular Chemistry, Academy of Science of the Czech Republic, Prague, Czech Republic*
[3]*Faculty of Chemical Technology, Institute of Applied Physics and Mathematics, University of Pardubice, Pardubice, Czech Republic*

Received 25 January 2011; accepted 2 July 2011
DOI 10.1002/app.35165
Published online 20 October 2011 in Wiley Online Library (wileyonlinelibrary.com).

ABSTRACT: To study the effect of organophilic clay concentration on nonisothermal crystallization, poly(L-lactic acid) (PLLA)/montmorillonite (MMT) nanocomposites were prepared by mixing various amounts of commercial MMT (Cloisite® 30B) and PLLA. The effect of MMT content on melting behavior and crystal structure of nonisothermal crystallized PLLA/MMT nanocomposites was investigated by differential scanning calorimetry (DSC), small-angle X-ray scattering, and wide-angle X-ray diffraction (XRD) analyses. The study was focused on the effect of the filler concentration on thermal and structural properties of the nonisothermally crystallized nanocomposite PLLA/MMT. The results obtained have shown that at filler loadings higher than 3 wt %, intercalation of the clay is observed. At lower clay concentrations (1–3 wt %), exfoliation predominates. DSC and XRD analysis data show that the crystallinity of PLLA/MMT composites increases drastically at high clay loadings (5–9 wt %). In these nanocomposites, PLLA crystallizes nonisothermally in an orthorhombic crystal structure, assigned to the α form of PLLA. © 2011 Wiley Periodicals, Inc. J Appl Polym Sci 124: 1643–1648, 2012

Key words: biopolymers; nanocomposites; crystal structures; DSC; X-ray

INTRODUCTION

Poly(L-lactic acid) (PLLA) is a relatively new biodegradable polymer primarily used for biomedical and packaging applications. It is an attractive polymer due to its performance characteristics and its biodegradability to harmless natural products at the end of its life cycle. It is a well-behaved thermoplastic with a reasonable shelf life for most single-use packaging applications. Depending on its disposal environment, it has a degradation time from several months to one hundred years. For conventional plastics, such as nylon, polypropylene, polyethylene, and polystyrene, this period can exceed 100 years. In terms of thermal and mechanical properties, PLLA is superior to other biodegradable polyesters. This is why, to reduce the impact on the environment, it is used as alternative to other commercial polymers.[1]

One of the features of semicrystalline polymers is that their lattice cell varies not only with temperature, but also strongly depends on crystallization conditions, annealing behavior, and plastic deformation.[2] In the literature, three crystalline modifications (α, β, and γ) of PLLA have been identified depending on preparation conditions.[3–8] The α-form is believed to grow during melt or cold crystallization and has a 10_3 helical chain conformation. Orthorhombic unit-cell parameters of the α form reported by different authors are varying in the intervals a = 10.78 − 10.5 Å, b = 6.45 − 6.04 Å, c (fiber axis) = 27.8 − 28.8 Å, depending on preparation conditions.[3,4,9,10] The β-form is prepared at high draw ratio and high drawing temperature and is known to take a left handed 3_1 helical conformation. A new γ-form has been obtained by epitaxial crystallization. Concerning the crystal structure of the α-form, there are two main opinions on the chain conformation of PLLA in the unit cell. The first one is the "pure" 10_3 helix regular (α) and the second one "distorted" 10_3 helix (α) influenced mainly by interchain interactions between CH_3 groups.[9,11] Recently, Zhang et al.[11] found that, depending on the crystallization temperature (T_c), the disorder and order phases of PLLA are formed at low (T_c < 100°C) and high (T_c > 120°C) temperatures, respectively. Apparently, the

Correspondence to: F. Ublekov (ublekov.philip@gmail.com).

Contract grant sponsors: Bulgarian Ministry of Education, Youth and Science, Czech Ministry of Education, Youth and Sports and Institute of Macromolecular Chemistry AS CR, v.v.i. of the Czech Republic, Prague.

different crystalline structures influence the physical and mechanical properties and degradation rates in polyesters. Therefore, a thorough understanding of the crystallization behavior and morphologies of PLLA is critical for its application. A number of studies on crystallization behavior and morphology of PLLA have been reported in literature, and the influence of nonisothermal and isothermal crystallization conditions on both crystallinity and microstructure was also studied.[11–14] Miyata and Masuko studied the nonisothermal crystallization of PLLA at various cooling rates. Samples cooled at rates higher than 10°C/min could not crystallize and remain amorphous. The amount of crystallinity developed in PLLA depends strongly on cooling rate.[9]

To overcome this problem, different nucleation agents (such as talc and clay) have been applied to enhance the overall crystallization rate of PLLA.[15] The addition of fillers is one of the most cost-effective methods to improve the physical properties of PLLA-based polymeric. The crystallization behavior of PLLA clay nanocomposites has also been studied to explore the effect of clay on the PLLA thermal and structural properties. Ray and Okamoto[16] have described the melt crystallization behavior of PLLA clay nanocomposites. They observed that the presence of clay increases the overall crystallization rate of PLLA. The clay particles act as a heterogeneous nucleating agent for PLLA melt crystallization in the nanocomposites. Similar effect has also been reported in other studies.[15,17–21] In the case of nonisothermal crystallization behavior of PLLA clay nanocomposites, Ogata considers that the clay has only minor nucleation effect, because the crystallization temperature does not depend on the clay content.[22]

Polymer-layered silicate nanocomposites have been the focus of academic and industrial attention in recent years, because the final composites often exhibit a desired enhancement of physical and chemical properties compared to the neat polymer matrix, even at very low clay contents. Montmorillonite (MMT) belongs to a family of clays known as smectites. Their crystal structure is formed by two fused silica tetrahedral sheets, sandwiched with an edge-shared octahedral sheet of either aluminum or magnesium hydroxide. The thickness of a single layer is about 1 nm, while the lateral size of the crystal can range from 30 nm to several microns or more. The silicate surface of MMT is relatively more hydrophilic than PLLA. Therefore, it has to be organically modified to compatibilize and facilitate its dispersion in PLLA.[23] Numerous works on polymers filled with layered silicates of different nature and properties have recently published.[24–30] It has been shown that at very low clay levels, the crystallization kinetics of the nanocomposites increased dramatically. Increasing the clay concentration above these levels results in decrease of the crystallization rate—in some cases, crystallization becomes even slower than that in the pure material. This behavior is commonly observed in filled polymers: at low filler concentration, the filler–polymer interfaces act as heterogeneous nucleating sites. In this way, the nucleation rate is increased and so is the crystallization kinetics. At higher filler loads, diffusion of polymer chains into the growing crystallites is hindered, which results in decreased overall crystallization rate. In most cases, crystallization behavior of these materials and PLLA has been investigated by performing isothermal crystallization tests and in a restricted composition range of clay.

Therefore, in this work, we intent to prepare nonisothermally crystallized PLLA/MMT nanocomposites and investigate their thermal and structural properties depending on various clay concentrations.

MATERIALS AND METHODS

PLLA Biomer® L-9000 (M_w = 160,000 g mol^{-1} and polydispersity index P_d = 3.6) with an L-isomer : D-isomer ratio of 98 : 02 was obtained from Biomer, Krailling, Germany. Molar masses were determined by GPC analysis (polystyrene standards). This material contains no additive or thermal stabilizer.

The organoclay used for the preparation of nanocomposites was commercial product, Cloisite 30B, purchased from Southern Clay Products, and it was used as received. According to the supplier, this 2 : 1 MMT contains quaternary ammonium ion with methyl tallow bis-2-hydroxyethyl (MT2EtOT) as organic modifier. Cloisite 30B organoclay and PLLA were dried under vacuum at 40 and 60°C, respectively, for at least 24 h. To study the effect of organophilic clay concentration on the crystallization, the PLLA/MMT nanocomposites were prepared by mixing PLLA with various amounts of MMT using melt-blending at 190°C in a Brabender extruder for 10 min. The nonisothermal crystallization of PLLA/MMT samples was carried out in the following way: the samples were placed between two steel plates and then first heated from room temperature to 190°C at the rates of 10°C/min and held for 5 min to eliminate the previous thermal history. After that, the samples were cooled to room temperature at a rate of 20°C/min. The samples were named as PLLA$_x$M, where x corresponds to the weight percentage of MMT in the composites. The same procedure was used for the preparation of neat PLLA sample.

Differential scanning calorimetry (DSC) analysis was carried out on a Perkin Elmer Pyris 1 DSC calorimeter cooled with liquid nitrogen and flushed with helium. Samples of about 10 mg were sealed in aluminum pans. The analysis was performed in three steps: first heating from 0 to 220°C at 10°C/min,

cooling from 220 to 0°C at −10°C/min, and second heating from 0 to 220°C at 10°C/min. Two-minute isothermal plateaux were inserted before, between, and after the ramps. The recorded exotherm/endotherm curves were evaluated as heats of crystallization/melting in joules per gram. Glass transition temperature was identified as a midpoint between the glassy and rubbery branches of the DSC trace and crystallization and melting temperatures as minima/maxima of the corresponding exotherm/endotherm plots.

The wide-angle X-ray diffraction (XRD) patterns were obtained using powder diffractometer HZG/4A (Freiberger Praezisionsmechanik GmbH, Freiberg). The Cu Kα radiation (λ = 1.54 Å) was used. Scanning range, 2θ = 1.4°–30° with step 0.1°. The geometrical arrangement of specimen with respect to X-ray source and counter for diffractometry was symmetrical (T/2T geometry).[31]

Small-angle X-ray scattering (SAXS) experiments were performed using a 3 pinhole camera (Molecular Metrology/Rigaku SAXS System) attached to a multilayer aspherical optics (Osmic/Rigaku Confocal MaxFlux), which, at the same time, monochromatizes as well as concentrates the beam of a microfocus X-ray tube (Bede microsource) operating at 45 kV and 0.66 mA (30 W). The camera was equipped with a multiwire, gas-filled area detector with an active area diameter of 200 mm (Gabriel design). The scattering curves were corrected for dark current and background. Intensities were q-calibrated using silver behenate. The scattering intensities were put on absolute scale using glassy carbon as the standard. Peak positions were used to obtain periodicities D according to Bragg's law, $D = 2\pi/q$; $q = (4\pi/\lambda)\sin\theta$, where λ is the wavelength and 2θ is the scattering angle.

RESULTS AND DISCUSSION

Thermal properties of the PLLA/MMT composites

DSC measurements were carried out in order to study the influence of the clay load on the thermal properties of the PLLA/MMT nanocomposites. Selected thermograms are presented in Figure 1.

All DSC data obtained are given in Tables I and II. Heat of cold crystallization ΔH_{cc} decreases with increasing MMT concentration due to reduced mobility of PLLA chains, resulting in retarded cold crystallization. Heat of melting, ΔH_m, which corresponds to the total crystallinity of the sample, shows the maximum for PLLA5M. The sum of these two values is proportional to the original crystallinity of the starting samples. The crystallinity of the neat polymer and nanocomposites was evaluated taking into account the amount of clay present in the nanocomposites, using the following equation[32]:

$$\chi_c[\%] = \frac{\Delta H_{cc} + \Delta H_m}{\Delta H_f\left(1 - \frac{\%\mathrm{wt}_{clay}}{100}\right)} \cdot 100$$

where ΔH_m is the specific melting enthalpy of the sample and $\%\mathrm{wt}_{clay}$ the weight percent of the clay in the sample. Different ΔH_f values can be found in the literature. The enthalpy of fusion calculated by Fisher et al.[33] is 93 J g^{-1}. Because the crystal density of PLLA (α-form) was estimated to be 1.285 g cm^{-3}, the enthalpy of fusion for a large crystal of infinity size corresponds to 135 J g^{-1}.[4,34] Glass transition temperature T_g is slightly higher for neat PLLA, which indicates that its chains are more closely packed in the glassy state; however, after crossing T_g, their mobility becomes higher (higher ΔH_{cc}). There is no trend in peak temperature of cold crystallization T_{cc}. The melting endotherm of neat PLLA shows single maximum reflecting uniform distribution of thickness of crystal lamellae. Melting endotherms of the PLLA/MMT samples show some secondary maxima or humps, pointing to multimodal distribution of lamellae. Similarly, to the first runs, the highest heat of cold crystallization ΔH_{cc} was found for neat PLLA. However, unlike the first runs, intensive cold crystallization was also detected for all PLLA/MMT samples. Heat of melting ΔH_m shows maximum for PLLA1M. If we assume that

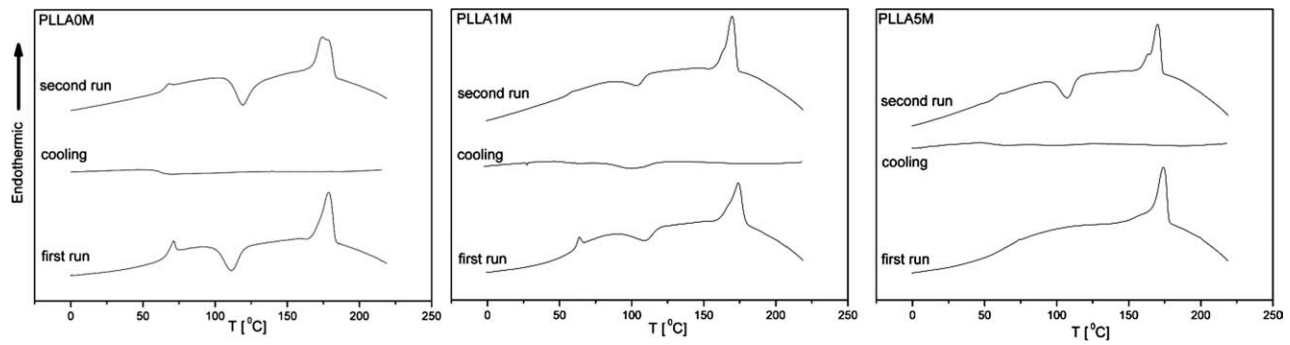

Figure 1 Selected DSC thermograms of PLLA and PLLA/MMT composites (first, second heating runs, and cooling).

TABLE I
Thermal Properties of PLLA\MMT Composites with Different MMT Load (Calculated form DSC Data)

	First heating run			Cooling	Second heating run		
Sample	ΔH_{cc} (J/g)	ΔH_m (J/g)	Δ	ΔH_{mc} (J/g)	ΔH_{cc} (J/g)	ΔH_m (J/g)	Δ
PLLA0M	−25.3	35.0	9.7	0	−33.9	34.5	0.6
PLLA1M	−17.9	37.5	19.6	−14.3	−12.6	43.5	16.6
PLLA3M	−15.2	38.8	23.6	−1.7	−25.5	36.4	9.2
PLLA5M	0	49.5	49.5	−2.4	−22.5	39.3	14.4
PLLA7M	0	42.1	42.1	−1.2	−23.1	36.4	12.1
PLLA9M	0	38.9	38.9	−3.4	−27.7	37.3	6.2

ΔH_m, the total melting enthalpy; ΔH_{cc}, the enthalpy of cold crystallization; ΔH_{mc}, the enthalpy of melt crystallization; $\Delta = \Delta H_{cc} + \Delta H_m$.

the samples after the first heating run are amorphous, the sum of the three values $\Delta H_{mc} + \Delta H_{cc} + \Delta H_m$ should be zero. This is, however, true for neat PLLA only. All PLLA/MMT samples show significant positive deviations. On melting during the first run, PLLA chains are released from the organized composite structure and subsequently undergo melt and cold crystallization during cooling and reheating. However, some chains still remain partially trapped in the composite structure and crystallize much slower. A flat exotherm of this slow crystallization is probably imposed under major part of the cooling and reheating traces and is not detected by DSC. It is also possible that keeping the samples at 220°C for 2 min after the first heating run is not sufficient for the complete removal of all crystallites, which then finally melt on reheating in the second run. Most probable is the combination of both these factors. To glass transition temperatures in the second runs applies the same as to those in the first runs. Higher T_g of neat PLLA also results in higher peak temperature of its cold crystallization T_{cc}. Melting endotherms of all samples in the second run show two peaks (or main peak and a hump) indicating bimodal distribution of lamellae. Both peaks of neat PLLA are found at significantly higher temperatures, which suggest higher perfection of the crystallites. From cooling runs, neat PLLA shows no exotherm of melt crystallization unlike the PLLA/MMT samples, where a pronounced maximum was found for heat of melt crystallization ΔH_{mc} of PLLA1M—its concentration of MMT is probably optimal for nucleation of melt crystallization. Glass transition temperature T_g is slightly higher for neat PLLA; its chains obviously pack more easily on cooling to reach the glassy state. No trend was found in peak temperature of melt crystallization T_{mc} of PLLA/MMT samples.

Structure of the PLLA/MMT composites

Figure 2 shows the XRD patterns of neat PLLA and PLLA/MMT nanocomposites in the range of $2\theta = 1.4°–30°$. The diffractogram of neat PLLA shows a broad maximum around $2\theta \sim 16°$, which confirms the amorphous structure of PLLA0M sample. However, for the PLLA1M and PLLA3M blends, a sharpening of the peak around 16° is observed. This indicates that PLLA is susceptible to some structural ordering after nonisothermal crystallization. The area of this peak is negligible in comparison with the amorphous halo. For this reason, the crystallinity

TABLE II
Values of Temperatures of PLLA\MMT Composites with Different Weight Ratio of MMT Collected form DSC Thermograms

	First run						Cooling		Second run			
			T_m (°C)								T_m (°C)	
Sample	T_g (°C)	T_{cc} (°C)	1	2	3	4	T_g (°C)	T_{mc} (°C)	T_g (°C)	T_{cc} (°C)	1	2
PLLA0M	65.9	111.4	–	–	178.7	–	61.5	–	64.4	119.4	175.5	178.0
PLLA1M	60.4	109.7	166.0	174.0	–	–	54.3	100.1	56.3	103.9	163.0	169.7
PLLA3M	61.7	110.0	–	173.5	178.6	–	58.4	96.5	59.5	112.2	166.2	172.5
PLLA5M	63.8	–	157.0	174.0	–	–	55.7	100.3	56.5	107.6	163.5	170.1
PLLA7M	62.2	–	158.4	173.6	178.0	193.7	57.3	97.5	59.6	107.0	165.0	171.6
PLLA9M	61.6	–	157.0	173.0	–	–	53.8	97.4	57.3	106.0	163.5	171.8

T_g, the glass transition temperature; T_{cc}, the temperature of cold crystallization peak; T_{m1}, T_{m2}, T_{m3}, and T_{m4}, temperatures of the melting peaks; T_{mc}, the temperature of melt crystallization peak.

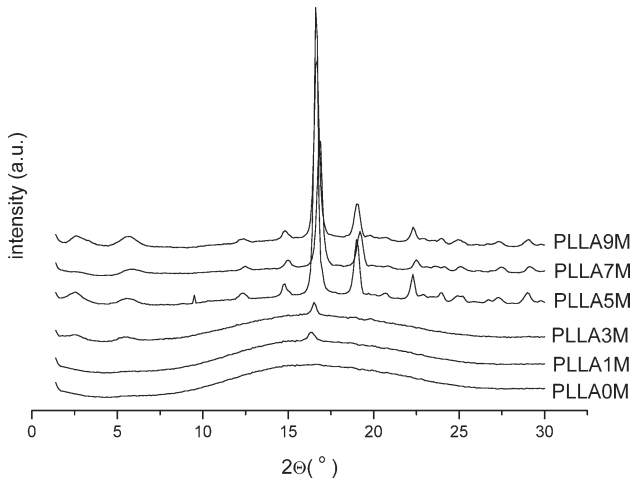

Figure 2 XRD patterns of PLLA and PLLA/MMT composites with different weight ratio.

is virtually zero. In contrast, the PLLA5M, PLLA7M, and PLLA9M composites are highly crystalline. The XRD patterns of these samples show many diffraction peaks, the position of which agrees well with the orthorhombic crystal structure, assigned as α-form.[3,4,10] The Miller indices of five intense diffraction peaks appearing at 12.4°, 14.8°, 16.7°, 19.1°, and 22.4° are (101), (010), (110)/(200), (111)/(201), and (102)/(210), respectively. The parameters of the calculated unit cell are $a = 10.55$ Å, $b = 5.91$ Å, $c = 9.42$ Å. Taking in account the results reported in the literature, we point out that the α-form can only be obtained upon isothermal crystallization or annealing process ($T_c > 120$ °C). With the presence of clay in PLLA matrix, samples with high loading show no shift in diffraction peaks, indicating that there is no significant effect on the polymorphism of the polymer. The unit-cell dimensions of the PLLA/MMT samples are not affected by the presence of clay. It has been reported that another distorted form, ά-form crystal, is observed for PLLA, and the characteristic diffraction peak of ά-crystal is detected at $2\theta = 25.5°$.[9,11] However, in this work, no evidence shows the formation of ά-form.

For Cloisite 30B, the XRD pattern shows four main peaks at 4.8°, 9.0°, 19.6°, and 24.0°. The intensity of these peaks is much lower in comparison with the reflection of the α-form due to the low concentration of MMT. The structure of nanocomposites is demonstrated by the enlargement degree of d_{001}-spacing distance. The d-spacing distance can be determined by the diffraction peak of the position d_{001} in the XRD pattern. The shift of the diffraction peak from $2\theta = 4.8°$ ($d = 18.3$ Å) in Cloisite 30B to $2\theta = 2.5°$ ($d_{001} = 35.3$ Å) in PLLA/MMT samples indicates intercalation of PLLA chains between silicate layers. The position of the second peak at 5.5° in the XRD pattern corresponds to the second order of the peak of intercalated structure. The blend

TABLE III
Structure Parameters of PLLA\MMT Composites

Sample	q_{max} (Å^{-1})	$L(q_{max})$ (Å)	χ_{dsc} (%)	χ_{xrd} (%)	L_c (Å)
PLLA0M	–	–	7	–	–
PLLA1M	–	–	15	–[a]	–
PLLA3M	0.0251	250	18	–[a]	–
PLLA5M	0.0290	216	39	66	142
PLLA7M	0.0270	232	34	58	134
PLLA9M	0.0265	237	32	51	120

PLLA0M and PLLA1M do not exhibit a maximum in the Lorentz corrected intensity profile. χ_{dsc}, crystallinity estimated by DSC (first heating run), $\Delta H_f = 135$ J g^{-1}; χ_{xrd}, crystallinity estimated by XRD; L_c, the lamellar thickness according to Kavesh and Schultz equation.[35]

[a] According XRD patterns, the crystallinity is virtually zero.

PLLA1M is exfoliated. The peak d_{001} of MMT characterizing silicate layers periodicity has disappeared. This indicates that the original structure of MMT with silicate layers stacks was destroyed.

The calculation of crystallinity was performed by using the software OriginLab®. The data from $2\theta = 7.5°$–30° were used. These results are given in Table III. The degree of crystallinity of the sample with 5 wt % clay loading is the highest according to the results from both XRD and DSC. With increasing the clay loadings results in a minor decrease in degree of crystallinity. Actually, the decrease of crystallinity is usually observed in the melt crystallization process of many polymers including PLLA.[15–22] This minor alteration is due to the inability of polymers chains to be fully incorporated into crystal structures. The presence of high clay loadings of dispersed clay prevents forming of large crystalline domains. This leads to smaller crystalline structure and more defect crystalline lamellae as well as less-ordered crystals.

To study the morphologies of PLLA and PLLA/MMT nanocomposites after nonisothermal crystallization, SAXS measurements were performed. Figure 3 shows the Lorentz-corrected SAXS profiles of

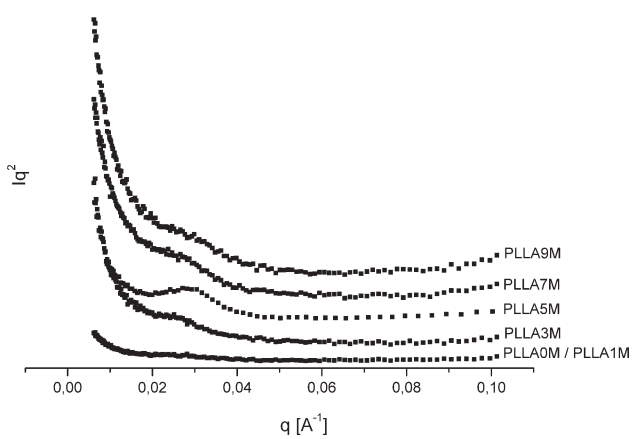

Figure 3 Lorentz-corrected SAXS profiles for the PLLA and its nanocomposites after nonisothermal crystallization.

nonisothermally crystallized PLLA and PLLA/MMT composites. The q_{max} values obtained from the Lorentz-corrected SAXS profiles are summarized in Table III. As seen in Figure 3, PLLA0M and PLLA1M no explicit diffraction peaks were observed, that is, they were amorphous, in consistent with the results obtained by XRD (see Fig. 2). On the contrary, diffraction peaks are detected for samples with 3, 5, 7, and 9 wt % clay loading. It is common practice to extract lamellar structure parameters from SAXS data of semicrystallinie polymers. In general, standard analysis yields the first the long period L (i.e., the mean distance between adjacent lamellae) as well as the lamellar thickness L_c. The long period was determined from the position q_{max} of the peak maximum in Lorentz-corrected SAXS profiles. The L values obtained in the present study are in good agreement with these reported in the literature—Huang et al.[36] 190–240 Å for PLLA film (M_w = 130,000 g mol^{-1}) crystallized at T_c = 120–148°C, 217 Å reported by Kawai et al.[37] for PLLA (M_w = 210,000 g mol^{-1}) crystallized at T_c = 120°C, 200–250 Å reported by Baratian et al.[38] for PLLA (M_w = 130,000 g mol^{-1}) crystallized at T_c = 120–145°C. The molecular weight of PLLA used in present study M_w = 160,000 g mol^{-1}. This value is very close to the data already given. The lamellar thickness L_c values are higher than those from the literature. Such results have to be attributed to unusual higher degree of crystallinity of those samples. The degrees of crystallinity values, estimated from XRD, are higher than the values found in the literature even for isothermal or nonisothermal crystallized PLLA.[11–15,17–21,39] The large experimental values for the degree of crystallinity have to be attributed to the intercalated clay structure and reduced heat of cold crystallization in those systems.

CONCLUSIONS

In the present study, we investigated the effects of organophilic MMT (Cloisite 30B) on nonisothermal crystallization of PLLA. The XRD results obtained have shown that, at filler loadings higher than 3 wt %, intercalation of the clay with polymer matrix is observed. At lower clay concentrations, exfoliation dominates. DSC and XRD analysis data show that the crystallinity of PLLA/organoclay composites increases remarkably at clay loadings higher than 5 wt %. Thermal measurements reveal that in neat PLLA, PLLA 1 wt % MMT, and PLLA 3 wt % MMT nanocomposites, cold crystallization takes place. In nanocomposites with 5, 7, and 9 wt % clay loading, the heat of cold crystallization disappears. This phenomenon has to be attributed to hindered PLLA chains movement in the clay galleries. In nanocomposite samples containing 1 and 3 wt % of clay, the reduced mobility of PLLA chains leads to decreased enthalpy of cold crystallization. On melting during the first run, PLLA chains are released from the organized composite structure and subsequently undergo melt and cold crystallization during cooling and reheating. PLLA/MMT nanocomposites nonisothermally crystallize in an orthorhombic crystal structure, which has been assigned as α form of PLLA. This significant alteration of the PLLA crystallization behavior has to be definitely attributed to the presence of Cloisite 30B organophilic clay in the system.

References

1. Urayama, H.; Kanamori, K. Macromol Mater Eng 2001, 286, 705.
2. Baltá-Calleja, F. J.; Vonk, C. G. In X-Ray Scattering of Synthetic Polymers; Elsevier: Amsterdam, 1989.
3. De Santis, P.; Kovacs, A. J. Biopolymers 1968, 6, 299.
4. Hoogsteen, W.; Postema, A. R.; Pennings, A. J. Macromolecules 1990, 23, 634.
5. Puiggali, J.; Ikada, Y.; Lotz, B. Polymer 2000, 41, 8921.
6. Pan, P.; Inoue, Y. Prog Polym Sci 2009, 34, 605.
7. Auras, R.; Harte, B.; Selke, S. Macromol Biosci 2004, 4, 835.
8. Zhang, J.; Duan, Y.; Sato, H.; Tsuji, H.; Noda, I. Macromolecules 2005, 38, 8012.
9. Miyata, T.; Masuko, T. Polymer 1997, 38, 4003.
10. Kobayashi, J.; Asahi, T.; Ichiki, M. J Appl Phys 1995, 77, 2957.
11. Zhang, J.; Tashiro, K.; Tsuji, H. Macromolecules 2008, 41, 1352.
12. Miyata, T.; Masuko, T. Polymer 1998, 39, 5515.
13. Di Lorenzo, M. L. Polymer 2001, 42, 9441.
14. Wu, D.; Wu, L.; Xu, B. J Polym Sci Part B: Polym Phys 2007, 45, 1100.
15. Pluta, M. J Polym Sci Part B: Polym Phys 2006, 44, 3392.
16. Nam, J. Y.; Ray S. S.; Okamoto, M. Macromolecules 2003, 36, 7126.
17. Hongbo, L.; Michel, A. H. Polymer 2007, 48, 6855.
18. Fujimori, A.; Masuko, T. Polym Eng Sci 2008, 48, 1103.
19. Krikorian, V.; Pochan, D. J. Macromolecules 2005, 38, 6520.
20. Paul, M.; Alexander, M. Polymer 2003, 44, 443.
21. Pluta, M.; Boitenx, G. Eur Polym J 2007, 43, 2819.
22. Ogata, N.; Jimenez, G.; Kawai, H. J Polym Sci Part B: Polym Phys 1997, 35, 389.
23. Ray, S.; Okamoto, M. Prog Polym Sci 2003, 28, 1539.
24. Ublekov, F.; Baldrian, J. J Polym Sci Part B: Polym Phys 2009, 47, 751.
25. Gopakumar, T.G.; Lee, J. A.; Kontopoulou, M.; Parent, J. S. Polymer 2002, 43, 5483.
26. Liu, X.; Wu, Q. Eur Polym J 2002, 38, 1383.
27. Liu, X.; Wu, Q.; Berglund, L. A. Polymer 2002, 43, 4967.
28. Wu, Z.; Chixin, Z.; Zhu, N. Polym Test 2002, 21, 479.
29. Li, J.; Zhou, C.; Gang, W. Polym Test 2003, 22, 217.
30. Tseng, C. R.; Wu, J. Y.; Lee, H. Y.; Chang, F. C. Polymer 2001, 42, 10063.
31. Alexander, L. E. In X-Ray Diffraction Methods in Polymer Science; Wiley: New York, 1969.
32. Fukushima, K.; Tabuani, D.; Camino, G. Mater Sci Eng C 2009, 29, 1433.
33. Fisher, E. W.; Sterzel, H. J.; Wenger, G.; Kolloid, Z. Z. Polymere 1973, 251, 980.
34. Miyata, T.; Masuko, T. Polymer 1983, 24, 175.
35. Kavesh S.; Schultz, J. M. J Polym Sci 1971, 9, 85.
36. Huang, J.; Runt, J. Macromolecules 1998, 31, 2593.
37. Kawai, T.; Rahma, N.; Matsuba, G. Macromolecules 2007, 40, 9463.
38. Baratian, S.; Hall, E. S.; Xu, R. Macromolecules 2001, 34, 4857.
39. Mano, J.; Wang, Y.; Viana, J. Macromol Mater Eng 2004, 289, 910.